

Assessment of DNA integrity in bovine viral diarrhea virus-infected cells using alkaline single-cell gel electrophoresis

Aidin Rahim Tayefeh*

Department of Animal Biotechnology, Faculty of Agricultural Biotechnology, National Institute of Genetic Engineering and Biotechnology, Tehran, Iran.

Article Info	Abstract
Article history: Received: 21 April 2025 Accepted: 10 December 2025 Available online: 15 April 2026	<p>Bovine viral diarrhea virus is a pestivirus of the <i>Flaviviridae</i> family including two biotypes, cytopathic (CP) and non-CP (NCP). This study aimed to evaluate DNA damage and apoptosis in Madin-Darby bovine kidney cells following infection with both biotypes. The MDBK monolayers were inoculated with a final dose of virus (1.00×10^3 Tissue Culture Infectious Dose 50% mL⁻¹) and incubated for 24 hr. DNA strand integrity was assessed using alkaline single-cell gel electrophoresis, and DNA damage was quantified through tail moment and olive tail moment indices (n = 3). Apoptosis was evaluated using annexin V-fluorescein isothiocyanate/propidium iodide flow cytometry to determine early and late apoptotic cell populations. Both biotypes significantly increased DNA fragmentation compared to the control group. The tail moment values were 15.89 ± 2.13 (control), 57.63 ± 16.20 (NCP), and 68.15 ± 9.93 (CP); while, olive tail moment values were 8.71 ± 1.01 (control), 29.35 ± 9.18 (NCP), and 35.14 ± 6.90 (CP). Apoptosis analysis showed a higher percentage of apoptotic cells in infected groups, with CP biotype of bovine viral diarrhea virus inducing the greatest early and late apoptotic responses, being consistent with its CP nature. Overall, both biotypes caused notable genomic injury and apoptosis in Madin-Darby bovine kidney cells, with CP producing the highest level of damage, confirming single-cell gel electrophoresis combined with apoptosis assays as sensitive tools for detecting virus-mediated genomic instability and supporting their potential application in breeding programs aimed at enhancing resistance to infectious diseases.</p>
Keywords: Apoptosis Bovine viral diarrhea virus DNA integrity Madin-Darby bovine kidney cells Single cell gel electrophoresis	

© 2026 Urmia University. All rights reserved.

Introduction

Bovine viral diarrhea (BVD) is one of the most economically important viral diseases affecting cattle worldwide, primarily due to its detrimental impact on fertility, fetal development, immunosuppression, and overall herd productivity.¹ The BVD virus (BVDV), a member of the *Flaviviridae* family and *pestivirus* genus, exists in two biotypes, cytopathic (CP) and non-CP (NCP), differing markedly in their interactions with host cells and their pathogenic consequences. The NCP biotype is responsible for establishing persistent infection, whereas the CP biotype is associated with overt CP effects and acute mucosal disease.^{2,3}

Genomic integrity is essential for normal cellular function, successful reproduction, and long-term health in livestock. Viral infections are known to disrupt this stability by altering DNA repair pathways, inducing DNA breaks and triggering chromosomal abnormalities.⁴ Recent studies suggest that BVDV infection may modulate

genes involved in DNA damage response and repair mechanisms, thereby increasing the susceptibility of infected cells to genomic instability.⁵ Understanding these mechanisms is crucial for developing diagnostic and therapeutic strategies aimed at reducing the genetic burden associated with BVD infection in cattle.

Apoptosis plays a central role in host-virus interactions and serves as an early indicator of cellular stress and genotoxic insult.⁶ Many viruses, like BVDV, either induce or suppress apoptosis depending on their replication strategy. Thus, apoptosis assessment is an important first step before evaluating downstream DNA damage.⁷ In the present study, apoptosis was first quantified using flow cytometry (annexin V/Propidium Iodide), followed by the alkaline single-cell gel electrophoresis assay, a technique for detecting single- and double-strand DNA breaks, alkali-labile sites, cross-links, and incomplete repair events at the single-cell level, to directly measure DNA strand breaks and genomic instability.⁸

*Correspondence:

Aidin Rahim Tayefeh. DVSc

Department of Animal Biotechnology, Faculty of Agricultural Biotechnology, National Institute of Genetic Engineering and Biotechnology, Tehran, Iran

E-mail: tayefe@nigeb.ac.ir



This work is licensed under a Creative Commons Attribution-NonCommercial-ShareAlike 4.0 International (CC BY-NC-SA 4.0) which allows users to read, copy, distribute and make derivative works for non-commercial purposes from the material, as long as the author of the original work is cited properly.

Materials and Methods

All chemicals and reagents were obtained from Sigma-Aldrich (St. Louis, USA) unless otherwise specified. The CP and NCP biotypes of BVDV, as well as Madin-Darby bovine kidney (MDBK) cells, were kindly provided by the Razi Vaccine and Serum Research Institute, Karaj, Iran. This study did not involve human participants or live animals. All procedures were conducted using established *in vitro* cell culture techniques. Therefore, ethics approval was not required.

Virus preparation. The BVDV biotypes were propagated in MDBK cells seeded in T-25 tissue culture flasks (Orange Scientific, Braine-l'Alleud, Belgium), containing Dulbecco's modified Eagle medium (DMEM; Gibco, ThermoFisher Scientific, Waltham, USA) supplemented with 10.00% fetal bovine serum (Gibco). Following four sequential passages, the culture supernatant was harvested, aliquoted, and stored at $-80.00\text{ }^{\circ}\text{C}$ until use. Virus titration was performed using the Reed method.⁹ Briefly, a frozen aliquot of the virus stock was thawed and subjected to serial 10-fold dilutions (1.00×10^{-4} to 1.00×10^{-8}) in serum-free Dulbecco's modified Eagle medium. Each dilution was inoculated in quadruplicate into 96-well cell culture plates (SPL Life Sciences, Pocheon-si Korea), containing MDBK monolayers. After 72 hr of incubation, wells were examined for viral CP effects (Fig. 1).

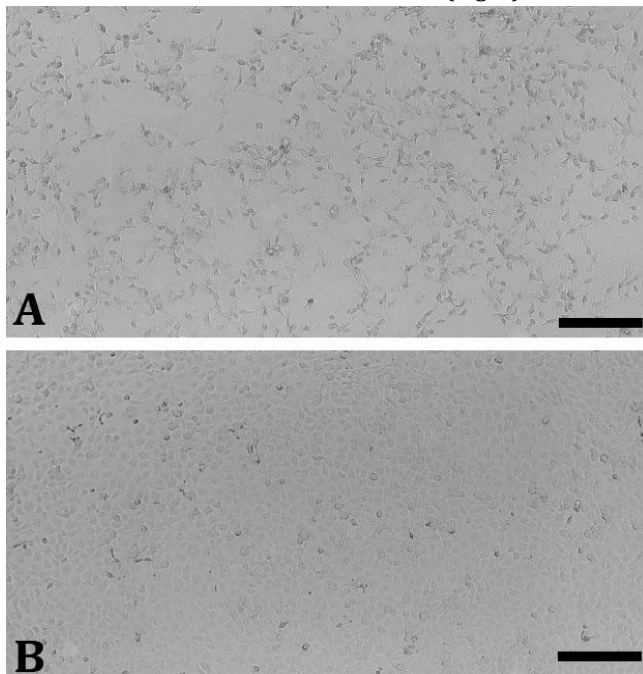


Fig. 1. A) Morphological cytopathic (CP) effects induced by bovine viral diarrhea virus biotypes in the Madin-Darby bovine kidney cells. The CP-infected cells show pronounced degeneration, cellular rounding, and detachment. **B)** Non-CP-infected cells maintain an overall intact monolayer, although intra-cytoplasmic inclusion bodies are visible, indicating viral replication despite the absence of overt CP changes (Scale bars = 200 μm).

Cell culture. The MDBK cells were maintained in Dulbecco's modified Eagle medium supplemented with 10.00% fetal bovine serum under standard incubation conditions ($37.00\text{ }^{\circ}\text{C}$, 5.00% CO_2 , and a humidified atmosphere). Cells were kept in the exponential growth phase (approximately 80.00% confluency), and the control group consisted of cells cultured in virus-free medium. In the treatment groups, cells were infected with either the CP or NCP biotype of BVDV. The final viral concentration selected for all subsequent experimental assays was 1.00×10^3 tissue culture infectious dose 50.00% (TCID₅₀) mL^{-1} .

Flow cytometric analysis. Apoptosis was assessed using the Annexin V- Fluorescein Isothiocyanate/ Propidium Iodide (annexin V-FITC/PI) dual-staining assay, as previously described.⁷ Following treatment, MDBK cells were harvested, washed with phosphate-buffered saline (1.00 X, 10.00 mM, and pH: 7.40), and centrifuged at 1,500 rpm for 5 min. The pellet was re-suspended in 1 \times binding buffer (Annexin V Binding Buffer; BioLegend, San Diego, USA) and staining controls were prepared (unstained, annexin V only, PI only, and annexin V + PI). For test samples, 3.00 μL annexin V-FITC (Annexin V-FITC Apoptosis Detection Kit, BioLegend) was added and incubated for 15 min at $4.00\text{ }^{\circ}\text{C}$ in the dark, followed by re-suspension in fresh binding buffer. Immediately before acquisition, 3.00 μL PI (BioLegend) was added. Samples were analyzed using a BD FACSCalibur™ flow cytometer (BD Biosciences, San Jose, USA), detecting FITC in Fluorescence Channel 1 - Height (FL1-H) and PI in FL3-H channels. The assay allowed discrimination of viable, early apoptotic, late apoptotic, and necrotic cells.

Quantification of DNA damage. The single-cell gel electrophoresis assay was performed to assess DNA strand breaks in MDBK cells following BVDV infection according to the method of Singh *et al.*, with minor modifications (Fig. 2).⁸ A layer of 1.00% normal-melting-point agarose (Sigma-Aldrich) in phosphate-buffered saline (1.00 X, 10.00 mM, and pH: 7.40) was first prepared on pre-cleaned slides at $65.00\text{ }^{\circ}\text{C}$. Approximately 1.00×10^5 cells were mixed with 0.50 -1.00% low-melting-point agarose (Sigma-Aldrich) in phosphate-buffered saline at $37.00\text{ }^{\circ}\text{C}$ and immediately pipetted onto the agarose-coated slides. After solidification at $4.00\text{ }^{\circ}\text{C}$, the slides were immersed in an ice-cold lysis solution, containing 2.50 M NaCl, 100 mM Ethylenediaminetetraacetic acid, 10.00 mM Tris-HCl, 1.00% Triton X-100, and 10.00% dimethyl sulfoxide (pH: 10.00), and kept for 1 - 2 hr at $4.00\text{ }^{\circ}\text{C}$ to remove membranes and intra-cellular proteins. Following lysis, the slides were equilibrated in freshly prepared alkaline electrophoresis buffer (300 mM NaOH and 1.00 mM ethylenediaminetetraacetic acid disodium; pH > 13.00) for 20 - 30 min to unwind DNA and reveal alkali-labile sites. Electrophoresis was performed by adjusting the buffer height to 2.00 - 3.00 mm above the gel surface and applying 0.78 V cm^{-1} ($\sim 300\text{ mA}$) for 15-20 min in the

dark at 4.00 °C. After electrophoresis, the slides were washed three times for 5 min each with 0.40 M Tris-HCl (pH: 7.50), gently air-dried, and stained with 4',6-diamidino-2-phenylindole (DAPI; 1.00 µg mL⁻¹ in distilled water). The stained nucleoids were examined under a fluorescence microscope (Eclipse E600; Nikon Corp., Tokyo, Japan) equipped with an appropriate filter set. Quantitative image analysis was performed using the OpenComet Software (version 1.3; an ImageJ plugin developed by Benjamin Gyori, Boston, USA). A total of 90 nucleoids *per* group (n = 3) were classified. Tail moment (TM) was calculated as the product of tail length and the percentage of DNA in the tail, while olive tail moment (OTM) was determined as the product of the tail DNA fraction and the distance between the centers of mass of the head and tail.

Damage index (DI). Damage index was assigned based on nucleoid morphology, where cells were scored into five classes (0 - 4) according to the head-tail ratio and tail extent as follows: 0 = undamaged DNA, 1 = minimal migration (head-tail ratio ≤ 1.00), 2 = moderate migration (1.00- 2.00), 3 = extensive migration (≥ 2.00), and 4 = complete migration with an unidentifiable head. The DI for each sample was calculated using the following formula:¹⁰

$$DI = (n_0 \times 0) + (n_1 \times 1) + (n_2 \times 2) + (n_3 \times 3) + (n_4 \times 4)$$

The DI value therefore ranges from 0 (all cells in class 0; no damage) to 400 (all 100 cells in class 4; maximal damage). The DI was used as an integrated, semi-quantitative indicator of overall DNA damage in each treatment group.

Statistical analysis. Statistical analyses were performed using SPSS Software (version 26.0; IBM Corp., Armonk, USA). Data were expressed as mean ± standard deviation. Prior to comparative analyses, the normality of data distribution was assessed using the Shapiro-Wilk test. Differences among experimental groups were evaluated using one-way analysis of variance, followed by Tukey's *post hoc* test for multiple comparisons. The *p* ≤ 0.05 was considered statistically significant. To determine significant apoptotic responses, the combined proportion of early (Q3) and late (Q2) apoptotic cells at each treatment condition was statistically compared with the live cells (Q4).

Results

Flow cytometric analysis. Flow cytometric evaluation of apoptosis revealed clear differences among MDBK cells exposed to the two BVDV biotypes. Control cells exhibited a predominantly viable population (86.10%; Q4), with low early (9.92%; Q3) and late apoptosis (3.42%; Q2), and negligible necrosis (0.60%; Q1), confirming normal membrane integrity and the absence of detectable cell death (Fig. 3). Cells infected with the NCP biotype showed a distinct shift toward early apoptosis, reflected by an increase in annexin V-positive/PI-negative cells (59.40%; Q3). The proportions of late apoptotic (7.44%; Q2) and necrotic cells (0.55%; Q1) were only modestly elevated, while viable cells decreased to 32.60% (Q4). This pattern indicates activation of apoptotic signaling without extensive membrane breakdown, being consistent with the NCP replication strategy (Fig. 3).

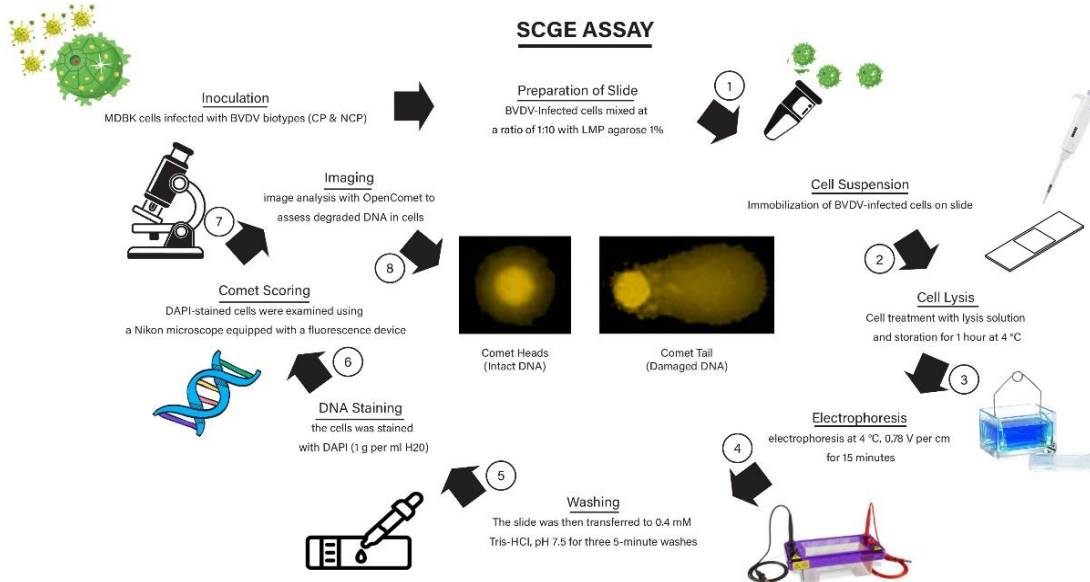


Fig. 2. Stepwise schematic workflow of the alkaline single-cell gel electrophoresis (SCGE) assay performed on the Madin-Darby bovine kidney (MDBK) cells infected with bovine viral diarrhea virus (BVDV) biotypes. The procedure includes preparation of infected cell suspensions, lysis, electrophoresis under alkaline conditions, washing, DAPI staining, comet scoring, and imaging for the assessment of DNA damage.

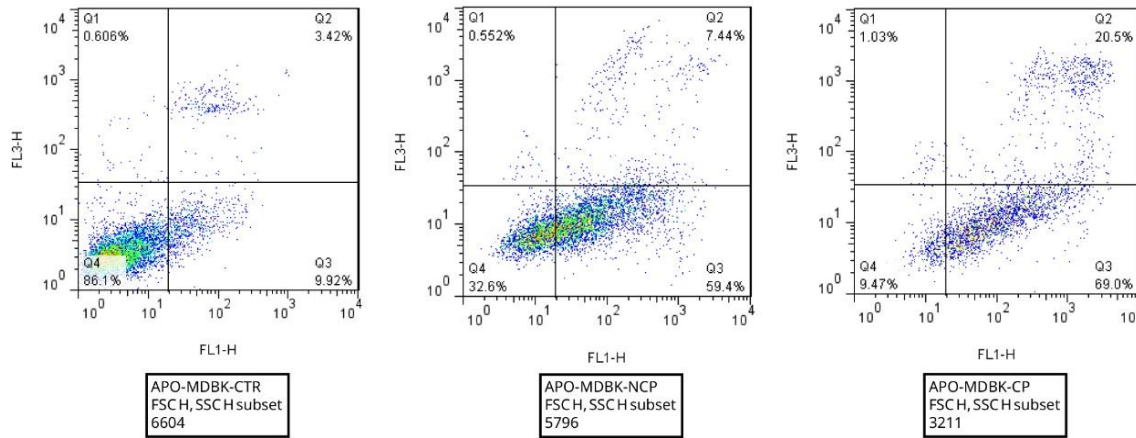


Fig. 3. Flow cytometric analysis of apoptosis in the Madin-Darby bovine kidney (MDBK) cells infected with bovine viral diarrhea virus biotypes. Dot plots illustrate live cells (Q4), early apoptotic cells (Q3), late apoptotic cells (Q2), and necrotic cells (Q1). Compared to the negative control (CTR), the non-cytopathic (NCP) biotype shows increased early apoptosis, while the cytopathic (CP) biotype demonstrates markedly higher levels of both early and late apoptotic populations.

In contrast, CP-infected cells demonstrated the most pronounced apoptotic alterations. Early apoptosis rose sharply to 69.00% (Q3), accompanied by substantial increases in late apoptosis (20.50%; Q2) and necrosis (1.03%; Q1). The viable cell population was markedly reduced to 9.47% (Q4), indicative of severe membrane disruption and progression toward secondary necrosis, being consistent with the cytolytic behavior of CP biotypes (Fig. 3). Collectively, the flow cytometry data show that NCP infection induces mild-to-moderate apoptosis, whereas CP infection triggers pronounced apoptotic and CP responses, highlighting the fundamental biological distinction between the two biotypes.

Quantification of DNA damage. Comet assay analysis revealed clear differences in DNA damage between the control and BVDV-infected groups after 24 hr (Fig. 4). As shown in Table 1, control cells exhibited the lowest levels of DNA migration, with TM and OTM values of 15.89 ± 2.13

and 8.71 ± 1.01 , respectively. In contrast, infection with both BVDV strains significantly increased DNA strand breaks compared to the control. The CP biotype of BVDV showed the highest levels of genotoxicity, with TM and OTM values of 68.15 ± 9.93 and 35.14 ± 6.90 , respectively.

Similarly, the NCP biotype of BVDV demonstrated elevated DNA damage with TM = 57.63 ± 16.20 and OTM = 29.35 ± 9.18 . Notably, both CP- and NCP-infected cells exhibited DNA fragmentation patterns similar to those observed in the positive control (doxorubicin; 1.00 μ M), clearly indicating a loss of DNA integrity in response to viral infection. Statistical analysis indicated that both infected groups differed significantly from the negative control ($p \leq 0.05$), whereas no significant difference was observed between the CP and NCP groups. These findings confirm that BVDV infection induces substantial DNA fragmentation in MDBK cells, with the CP strain producing slightly stronger genotoxic effects.

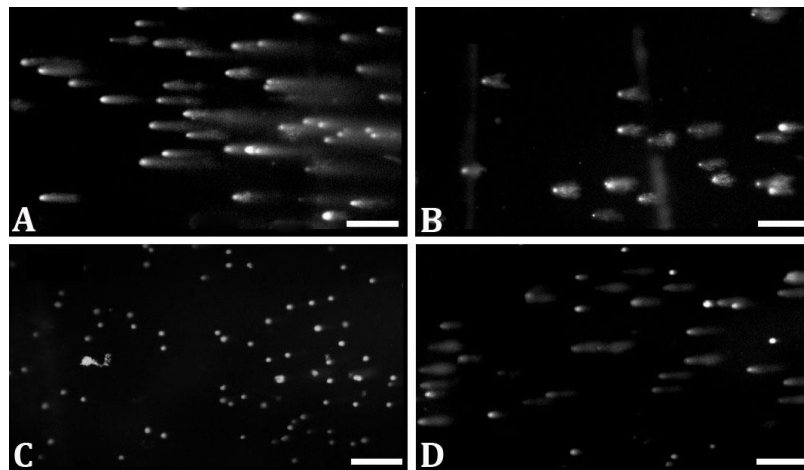


Fig. 4. Alkaline single-cell gel electrophoresis images of the Madin-Darby bovine kidney cells infected with bovine viral diarrhea virus biotypes. **A)** The cytopathic, and **B)** non-cytopathic groups show increased DNA migration compared to **C)** negative control. **D)** Doxorubicin (DOX; 1.00 μ M) was used as a positive control (Scale bars = 200 μ m).

Table 1. Quantification of DNA damage in bovine viral diarrhea virus (BVDV)-infected Madin-Darby bovine kidney (MDBK) cells. Data represent Mean \pm SD (90 comets *per* group; n = 3).

Groups	Time (hr)	TM	OTM
Control	24	15.89 \pm 2.13 ^a	8.71 \pm 1.01 ^a
Cytopathic BVDV	24	68.15 \pm 9.93 ^b	35.14 \pm 6.90 ^b
Non-cytopathic BVDV	24	57.63 \pm 16.20 ^b	29.35 \pm 9.18 ^b

Tail moment (TM) and olive tail moment (OTM) in MDBK cells following 24 hr infection with BVDV biotypes.

^{ab} Different superscript letters indicate significant differences at $p \leq 0.05$.

Damage index. Visual scoring of comets revealed a clear shift toward higher damage classes in infected groups. The control group showed the highest proportion of class 0 nuclei, while both BVDV-infected groups exhibited increased class 2.00-3.00 comets. The calculated DI values were 119 for the control, 214 for CP biotype of BVDV, and 211 for NCP biotype of BVDV, indicating that BVDV infection significantly increases DNA damage, with the CP strain producing slightly more severe genotoxicity (Table 2).

Table 2. Damage index (DI) in bovine viral diarrhea virus (BVDV)-infected Madin-Darby bovine kidney cells.

Groups	Class 0	Class 1	Class 2	Class 3	Class 4	DI (0-400)
Control	36	12	10	29	0	119
CP BVDV	1	15	22	49	2	214
NCP BVDV	0	14	32	39	4	211

Visual scoring distribution of 90 comets *per* group (n = 3) in five damage classes (0-4). The DI was calculated as the sum of number of nuclei in each class \times class value. The DI ranges from 0 (no damage) to 400 (maximum observable damage). Cytopathic (CP) and non-CP (NCP) biotypes of BVDV induced markedly higher DI values compared to the control group.

Discussion

The present study demonstrated that infection of MDBK cells with either CP or NCP biotypes of BVDV significantly compromised DNA integrity, as evidenced by increased TM, OTM, and DI values. The genotoxic changes observed here are consistent with previous findings indicating that BVDV infection interferes with genome maintenance. Elevated sister chromatid exchange frequency, fragile sites, and DNA strand breaks in BVDV-infected cattle have been reported previously, with single-cell gel electrophoresis identified as the most sensitive indicator of genomic instability. Additional genotoxicity assays, such as the micro-nucleus test, sister chromatid exchange analysis, and chromosomal aberration profiling, have also demonstrated that pestivirus infection leads to chromatid gaps, acentric fragments, aneuploidy, reduced mitotic index, and nuclear bud formation, all of which reflect impaired chromosome segregation and weakened DNA repair capacity.⁴ Similarly, our results showed substantial DNA fragmentation in both CP- and NCP-infected cells

compared to the negative controls, confirming the detrimental effect of BVDV on chromosomal integrity. The viral presence may induce ongoing replication-associated stress and hinder DNA repair pathways, resulting in sustained genotoxic pressure.

Apoptosis analysis further clarified the mechanistic differences between the two biotypes. The CP biotype of BVDV induced pronounced early and late apoptosis, being consistent with its lytic replication cycle and ability to trigger rapid host-cell destruction. In contrast, NCP biotype of BVDV predominantly increased early apoptosis while maintaining a higher proportion of viable cells. This finding agrees with previous reports indicating that NCP strains avoid extensive cytolysis to enable persistent infection.¹¹ Similar dual patterns have been documented in other viral systems. Papillomaviruses,¹² parvoviruses,¹³ and coronaviruses¹⁴ have been shown to induce considerable DNA damage even when apoptosis levels remain moderate, whereas lytic viruses, such as herpes simplex virus -1, produce both severe apoptosis and extensive DNA breakage.¹⁵ These comparisons reinforce the idea that the mode of viral replication critically shapes the balance between apoptosis and genotoxicity. In coronavirus disease 2019 patients, leukocyte DNA damage correlates with disease severity and clinical parameters, highlighting DNA injury as an informative biomarker.¹⁶ Similarly, parvovirus minute virus of mice exploits sites of DNA damage for replication, leading to genome instability,¹³ and herpes simplex virus -1 infection impairs neuronal DNA repair, resulting in both single- and double-strand breaks.¹⁵ Influenza virus also produces genotoxic and teratogenic effects, manifesting as chromosomal aberrations in cultured cells and peripheral blood leukocytes.¹⁷ When viewed collectively with our results, these studies demonstrate that virus-induced DNA damage is a conserved pathogenic mechanism across diverse viral families.

In conclusion, the present study demonstrates that both CP and NCP biotypes of BVDV compromise genomic integrity, although through distinct mechanisms. The CP biotype of BVDV causes extensive DNA damage primarily *via* apoptosis and cytopathic effects, while NCP biotype of BVDV induces a more persistent form of genotoxic stress under conditions of continued cellular viability. These mechanistic differences underscore the complex nature of BVDV-host interactions and highlight the relevance of DNA integrity biomarkers in assessing the pathogenic potential of pestiviruses. Future studies should aim to dissect the molecular pathways underlying BVDV-induced genotoxicity. Integrating assays, such as γ -H2AX foci quantification, Terminal deoxynucleotidyl transferase dUTP Nick End Labeling (TUNEL), and cytokinesis-block micro-nucleus testing, will provide deeper insights into double-strand break formation, repair deficiencies, and apoptosis-necrosis balance during infection. Additionally,

evaluating oxidative stress markers and DNA repair gene expression may help elucidate the contribution of replication stress and impaired repair systems. A clearer understanding of these processes could guide the development of genetic selection strategies, targeted antiviral therapies, or management practices aimed at reducing BVDV-associated reproductive losses in cattle.

Acknowledgments

The author expresses sincere appreciation to the National Institute of Genetic Engineering and Biotechnology, Tehran, Iran, for providing laboratory space, essential equipment, and technical facilities, enabled the completion of this research. This study received no external financial support. All experimental procedures and analyses were performed using the personal funding and institutional laboratory access provided to the author.

Conflict of interest

The author declares that no competing interests exist.

References

1. Elmore S. Apoptosis: a review of programmed cell death. *Toxicol Pathol* 2007; 35(4): 495-516.
2. Khodakaram-Tafti A, Farjanikish GH. Persistent bovine viral diarrhoea virus (BVDV) infection in cattle herds. *Iran J Vet Res* 2017; 18(3): 154-163.
3. Oguejiofor CF, Thomas C, Cheng Z, et al. Mechanisms linking bovine viral diarrhoea virus (BVDV) infection with infertility in cattle. *Anim Health Res Rev* 2019; 20(1): 72-85.
4. Kępka K, Wójcik E, Wysokińska A. Identification of genomic instability in cows infected with BVD virus. *Animals (Basel)* 2023; 13(24): 3800. doi: 10.3390/ani13243800.
5. Harutyunyan T, Sargsyan A, Kalashyan L, et al. DNA damage in moderate and severe COVID-19 cases: relation to demographic, clinical, and laboratory parameters. *Int J Mol Sci* 2024; 25(19): 10293. doi: 10.3390/ijms251910293.
6. Roulston A, Marcellus RC, Branton PE. Viruses and apoptosis. *Annu Rev Microbiol* 1999; 53: 577-628.
7. Rieger AM, Nelson KL, Konowalchuk JD, et al. Modified annexin V propidium iodide apoptosis assay for accurate assessment of cell death. *J Vis Exp* 2011; (50): 2597. doi: 10.3791/2597.
8. Singh NP, McCoy MT, Tice RR, et al. A simple technique for quantitation of low levels of DNA damage in individual cells. *Exp Cell Res* 1988; 175(1): 184-191.
9. Reed LJ. A simple method of estimating fifty per cent endpoints. *Am J Epidemiol* 1938; 27: 493-497.
10. Kobayashi H, Sugiyama C, Morikawa Y, et al. A comparison between manual microscopic analysis and computerized image analysis in the single cell gel electrophoresis assay. *MMS Commun* 1995; 3(2): 103-115.
11. Dzitsiuk V, Tipilo H. Chromosomal anomalies in dairy cattle as reasons of impaired fertility. *Agric Sci Pract* 2019; 1: 60-66.
12. Jones KM, Bryan A, McCunn E, et al. The causes and consequences of DNA damage and chromosomal instability induced by human papillomavirus. *Cancers (Basel)* 2024; 16(9): 1662. doi: 10.3390/cancers16091662.
13. Abrahams RR, Majumder K. Small genomes, big disruptions: parvoviruses and the DNA damage response. *Viruses* 2025; 17(4): 494. doi: 10.3390/v17040494.
14. Abiri E, Mirzaii M, Moghbeli M, et al. Investigating DNA damage caused by COVID-19 and influenza in post COVID-19. *Mamm Genome* 2025; 36(1): 200-212.
15. Çakar DA, Yirün A, Erdemli-Köse SB, et al. The combined effects of HSV-1 glycoprotein D and aluminum hydroxide on human neuroblastoma cells: insights into oxidative DNA damage, apoptosis, and epigenetic modifications. *Neurotoxicology* 2025; 108: 123-133.
16. Mihaljevic O, Zivancevic-Simonovic S, Cupurdija V, et al. DNA damage in peripheral blood lymphocytes of severely ill COVID-19 patients in relation to inflammatory markers and parameters of hemostasis. *Mutagenesis* 2022; 37(3-4): 203-212.
17. Kaleelullah RA, Garugula N. Teratogenic genesis in fetal malformations. *Cureus* 2021; 13(2): e13149. doi: 10.7759/cureus.13149.